

SANDIA REPORT

SAND2014-17401

Unlimited Release

Printed Month and Year

Wave Energy Converter (WEC) Array Effects on Wave, Current, and Sediment Circulation: Monterey Bay, CA

Craig Jones, Jason Magalen, and Jesse Roberts,

Prepared by
Sandia National Laboratories
Albuquerque, New Mexico 87185 and Livermore, California 94550

Sandia National Laboratories is a multi-program laboratory managed and operated by Sandia Corporation, a wholly owned subsidiary of Lockheed Martin Corporation, for the U.S. Department of Energy's National Nuclear Security Administration under contract DE-AC04-94AL85000.

Approved for public release; further dissemination unlimited.



Sandia National Laboratories



Issued by Sandia National Laboratories, operated for the United States Department of Energy by Sandia Corporation.

NOTICE: This report was prepared as an account of work sponsored by an agency of the United States Government. Neither the United States Government, nor any agency thereof, nor any of their employees, nor any of their contractors, subcontractors, or their employees, make any warranty, express or implied, or assume any legal liability or responsibility for the accuracy, completeness, or usefulness of any information, apparatus, product, or process disclosed, or represent that its use would not infringe privately owned rights. Reference herein to any specific commercial product, process, or service by trade name, trademark, manufacturer, or otherwise, does not necessarily constitute or imply its endorsement, recommendation, or favoring by the United States Government, any agency thereof, or any of their contractors or subcontractors. The views and opinions expressed herein do not necessarily state or reflect those of the United States Government, any agency thereof, or any of their contractors.

Printed in the United States of America. This report has been reproduced directly from the best available copy.

Available to DOE and DOE contractors from

U.S. Department of Energy
Office of Scientific and Technical Information
P.O. Box 62
Oak Ridge, TN 37831

Telephone: (865) 576-8401
Facsimile: (865) 576-5728
E-Mail: reports@adonis.osti.gov
Online ordering: <http://www.osti.gov/bridge>

Available to the public from

U.S. Department of Commerce
National Technical Information Service
5285 Port Royal Rd.
Springfield, VA 22161

Telephone: (800) 553-6847
Facsimile: (703) 605-6900
E-Mail: orders@ntis.fedworld.gov
Online order: <http://www.ntis.gov/help/ordermethods.asp?loc=7-4-0#online>



SAND2014-17401
Unlimited Release
Printed Month Year

Wave Energy Converter (WEC) Farm Effects on Wave, Current, and Sediment Circulation: Monterey Bay, CA

Craig Jones and Jason Magalen
Sea Engineering, Inc.
200 Washington Street, Suite 101
Santa Cruz, CA 95060

Jesse Roberts
Water Power
Sandia National Laboratories
P.O. Box 5800
Albuquerque, New Mexico 87185-MS1124

Abstract

The goals of this study were to develop tools to quantitatively characterize environments where wave energy converter (WEC) devices may be installed and to assess effects on hydrodynamics and local sediment transport. A large hypothetical WEC array was investigated using wave, hydrodynamic, and sediment transport models and site-specific average and storm conditions as input. The results indicated that there were significant changes in sediment sizes adjacent to and in the lee of the WEC array due to reduced wave energy. The circulation in the lee of the array was also altered; more intense onshore currents were generated in the lee of the WECs. In general, the storm case and the average case showed the same qualitative patterns suggesting that these trends would be maintained throughout the year. The framework developed here can be used to design more efficient arrays while minimizing impacts on nearshore environments.

ACKNOWLEDGMENTS

The research and development described in this document was funded by the U.S. Department of Energy. Sandia is a multiprogram laboratory operated by Sandia Corporation, a Lockheed Martin Company, for the United States Department of Energy's National Nuclear Security Administration under contract DE-AC04-94AL85000.

This research was made possible by support from the Department of Energy's Wind and Water Power Technologies Office.

CONTENTS

1. Introduction.....	9
2. Model Development and Application.....	11
2.1. Wave Model.....	11
2.1.1. Site-Specific Wave Model: Monterey Bay and Santa Cruz, CA.....	12
2.2. Wave Model Validation.....	14
2.2.1. Coarse Grid Monterey Bay Model Validation.....	14
2.2.2. Finer Grid Santa Cruz Model Validation.....	16
2.3. Hydrodynamic Model.....	17
2.3.1. Site-Specific Hydrodynamic Model: Monterey Bay and Santa Cruz, CA.....	19
2.4. Hydrodynamic Model Validation.....	21
3. Simulation of WEC Array.....	25
3.1. Wave Model with WECs.....	26
3.2. Hydrodynamics and Sediment Transport Models with WECs.....	27
4. Discussion and Conclusions.....	33
5. References.....	35
Distribution.....	37

FIGURES

Figure 1. Monterey Bay model domain. NOAA NDBC buoys used for model validation are shown in green.....	13
Figure 2. Santa Cruz model domain. Nearshore wave-measurement buoy and bottom-mounted ADCP measurement locations are shown for reference.....	14
Figure 3. Model (line) representing the wave height (H_s), peak wave period (T_p) and mean wave direction (MWD) obtained from the Monterey Bay SWAN model. Measured data (dots) were obtained from the NOAA NDBC buoy 46236 in Monterey Bay.....	15
Figure 4. Model (line) representing the wave height (H_s), peak wave period (T_p) and mean wave direction (MWD) obtained from the nearshore Santa Cruz SWAN model. Measured data (dots) were obtained from the Datawell DWR-G buoy deployed during the field study.....	17
Figure 5. Contours of bathymetry mapped to 20 m x 20 m SNL-EFDC grid for the Santa Cruz region.....	20
Figure 6. Tidal water levels and winds applied as model boundary conditions for the Santa Cruz model.....	21
Figure 7. Significant wave heights from the SWAN model in the SNL-EFDC model domain on 10/14/2009.....	22
Figure 8. Peak wave heights and velocity vectors in the model domain on 10/14/2009.....	22
Figure 9. Combined wave and current shear stresses and velocity vectors in the model domain on 10/14/2009.....	23
Figure 10. Model (line) representing the current magnitude obtained from the nearshore Santa Cruz SNL-EFDC model. Measured data (dots) were obtained from the Teledyne RDI ADCP deployed during the field study.....	23

Figure 11. Near-shore Santa Cruz, CA, model bathymetry and WEC device array location..... 25

Figure 12. Modeled wave heights prior to the installation of a WEC device array..... 26

Figure 13. Modeled wave heights after installation of a WEC device array for an incoming wave height of 1.7 m. 27

Figure 14. Velocity vectors and resultant sediment bed height change in cm from the combined wave and circulation model for the 3.5 m wave case. The top panel illustrates the baseline case and the bottom panel shows the case with the offshore WEC array in place. 29

Figure 15. Differences between the combined wave and circulation baseline model and WEC array model after 4 days of 1.7 m waves and normal tides. The top panel illustrates the change in sediment bed height and the bottom panel shows the change in sediment surface particle size. . 31

Figure 16. Differences between the combined wave and circulation baseline model and WEC array model after 4 days of 3.5 m waves and normal tides. The top panel illustrates the change in sediment bed height and the bottom panel shows the change in sediment surface particle size. . 32

TABLES

Table 1. Model error statistics for the Monterey Bay SWAN model. 16

Table 2. Model error statistics for the Santa Cruz SWAN model. 16

Table 3. Model error statistics for the Santa Cruz combined wave and current model. 24

Table 4. Sediment size class properties. 28

NOMENCLATURE

ADCP	Acoustic Doppler Current Profiler
CEROS	Center for Excellence in Ocean Science
CO-OPS	Center for Operational Oceanographic Products & Services
DOE	Department of Energy
D_p	Dominant wave direction
DWR-G	Datawell Directional Wave Buoy
EFDC	Environmental Fluid Dynamics Code
H_s	Significant wave height
ME	Mean error or bias
MHK	Marine hydrokinetic devices
MWD	Mean wave direction
NCEP	National Centers for Environmental Prediction
NDBC	National Data Buoy Center
NOAA	National Oceanic and Atmospheric Administration
NWW3	WaveWatch III
RMSE	Root mean square error
SI	Scatter index
SNL	Sandia National Laboratories
SWAN	Simulating WAVes Nearshore
T_p or T_s	Peak wave period
U.S. DoD	United States Department of Defense
U.S. EPA	United States Environmental Protection Agency
USGS	United States Geological Survey
WEC	Wave energy converter

1. INTRODUCTION

The physical environment characterization and commensurate alteration of an environment due to wave energy converter (WEC) devices, or arrays of devices, must be understood in order to make informed device-performance predictions, specifications of hydrodynamic loads, and environmental responses (e.g., changes to circulation patterns, sediment dynamics). The performance of wave-energy devices will be affected by nearshore waves and circulation primarily where WEC infrastructure (e.g., anchors, piles) are exposed to large forces from the surface-wave action and currents. Wave-energy devices will be subject to additional corrosion, fouling, and wearing of moving parts caused by suspended sediments in the overlying water. The alteration of the circulation and sediment transport patterns may also alter local ecosystems through changes in benthic habitat, circulation patterns, or other environmental parameters.

The goal of this study was to develop tools to quantitatively characterize the environments where WEC devices may be installed and to assess effects of WECs on hydrodynamics and local sediment transport. The primary tools described are wave, hydrodynamic, and sediment transport models. Sandia National Laboratories – Environmental Fluid Dynamics Code (SNL-EFDC; James et al., 2011), an extension of the United States Environmental Protection Agency (U.S. EPA) EFDC, provides a suitable platform for modeling the necessary hydrodynamics and has been modified to directly incorporate output from the Simulating WAVes Nearshore (SWAN) wave model. In order to ensure confidence in the resulting evaluation of system wide effects, the models were appropriately constrained and validated with measured data, where available. Here, a model is developed and exercised for a location in Monterey Bay, CA where a WEC array could be deployed.

2. MODEL DEVELOPMENT AND APPLICATION

Circulation and mixing in nearshore regions are controlled by nonlinear combinations of winds, tides, and waves. During a large wave event, wave effects can dominate the nearshore currents and mixing. The modeling approach for investigating WEC devices in the nearshore is structured to capture complex wave-induced currents and mixing, as well as tide- and wind-driven currents. This requires formulation and integration of both a wave model and a transport/circulation model. The final model results are ultimately linked to site-appropriate sediment properties to provide a full sediment transport model for investigating scour and suspended solids. The following sections outline the modeling components and application in Monterey Bay, CA.

2.1. Wave Model

The U.S. National Oceanic and Atmospheric Administration (NOAA) operational wave model, WaveWatch III (NWW3), was used to generate deepwater wave conditions offshore of the site. WaveWatch III is a third-generation wave model developed at the NOAA National Centers for Environmental Prediction (NCEP). It has been extensively tested and validated. For oceanic scales and deep water, NWW3 has proven to be an accurate predictor of wave spectra and characteristics and has therefore become the operational model of choice for NCEP and many other institutions.

The resolution, or grid spacing, of the NWW3 model was $1.00^\circ \times 1.25^\circ$ (degrees latitude by degrees longitude). This model was run using October 2009 winds as input boundary conditions. Daily wave parameters including significant wave height (H_s), peak wave period (T_p) and dominant wave direction (D_p) were obtained for a reference point located offshore. A nearshore wave-prediction model was nested with the NWW3 model to predict wave propagation into nearshore regions.

As deepwater waves approach the coast, they are transformed by processes including refraction (as they pass over changing bottom contours), diffraction (as they propagate around objects such as headlands), shoaling (as the depth decreases), energy dissipation (due to bottom friction), and ultimately, by breaking. The propagation of deepwater waves into each site was modeled using the open-source program SWAN (Simulating WAVes Nearshore), developed by Delft Hydraulics Laboratory, which has the capability of modeling all of these processes in shallow coastal waters. SWAN is a non-stationary (non-steady state) third-generation wave model, based on the discrete spectral-action balance equation that covers the total range of wave frequencies. Wave propagation is based on linear wave theory, including the effect of wave-generated currents. The processes of wind generation, dissipation, and nonlinear wave-wave interactions are represented explicitly with state-of-the-science third-generation formulations in SWAN.

SWAN can also be applied as a stationary (steady-state) model, which is acceptable for most coastal applications because the travel time of the waves from the seaward boundary to the coast is small compared to the time scale of variations in the incoming wave field, the wind, or the tide. SWAN provides many output quantities including two dimensional spectra, significant wave height, mean and peak wave period, mean wave direction, and directional spreading. The SWAN model has been successfully validated and verified in laboratory and complex field cases.

2.1.1. Site-Specific Wave Model: Monterey Bay and Santa Cruz, CA

The Santa Cruz, CA, coastal region was chosen for the model framework development due to the similarity to the complex environments where MHK devices would be installed. In addition, under the U.S. Department of Defense (DoD) Center for Excellence in Ocean Science (CEROS) research program, field data collection and model development in Santa Cruz, CA was leveraged for this task.

The NOAA operational wave model, NWW3, was used to generate deepwater wave conditions offshore of Monterey Bay, CA. Daily wave parameters, including H_s , T_p and D_p were obtained for a reference point located at 37.00°N latitude, -122.5°W longitude. A SWAN model was nested with the NWW3 model to predict the propagation of waves into Monterey Bay, CA, and nearshore Santa Cruz, CA.

The Monterey Bay SWAN model domain is shown in Figure 1. The SWAN model offshore boundary was 60 km offshore of central Monterey Bay (i.e. in open waters of the Pacific Ocean). NWW3 wind output was used to drive the Monterey Bay SWAN model because measured wind speeds were further onshore and, potentially, unrepresentative at this location. The NWW3 winds were predicted from a global wind speed model with the objective of predicting wind speeds in the open ocean. To validate the wind speeds used, the NWW3 wind predictions were compared with NOAA NDBC wind measurements to validate this assumption. Both waves and wind were outputted at 3 hour time intervals from NWW3. This was the corresponding update duration for the non-Stationary Monterey Bay SWAN model.

NOAA National Data Buoy Center (NDBC) data from station number 46236 were used to validate the model predictions for wave height, wave period, and mean wave direction. NDBC stations 46092 and 46091 were used to validate wind speed and direction. These stations were selected based on the type of data that each recorded (i.e., station 46236 did not record wind data but recorded wave height and period). Station 46240 was located in shallow water near the southern Monterey Bay coastline, in an area not considered acceptable for deepwater model validation; therefore, its data were not used.

Wave conditions from the Monterey Bay SWAN domain were outputted for a second nested model domain at a reference point 4 km south of Santa Cruz, CA. The coordinates of the output location were 36.9236°N, -122.0488°W. The grid resolution of the nested computational grid was approximately 0.0003° degrees in latitude and longitude ($25 \times 30 \text{ m}^2$ in x and y). The wave-spectrum boundary conditions were applied along the offshore (southerly) boundary of the Santa Cruz SWAN model domain. The model was run as a stationary model (no temporally varying wind-field updates). Winds were assumed to have minimal effect on the nearshore wave conditions due to the relatively short distance from the offshore model domain boundary to the coastline. The Santa Cruz SWAN model wave conditions were updated during the period of study (10/18/2009 to 10/25/2009) with the daily Monterey Bay SWAN model output spectra.

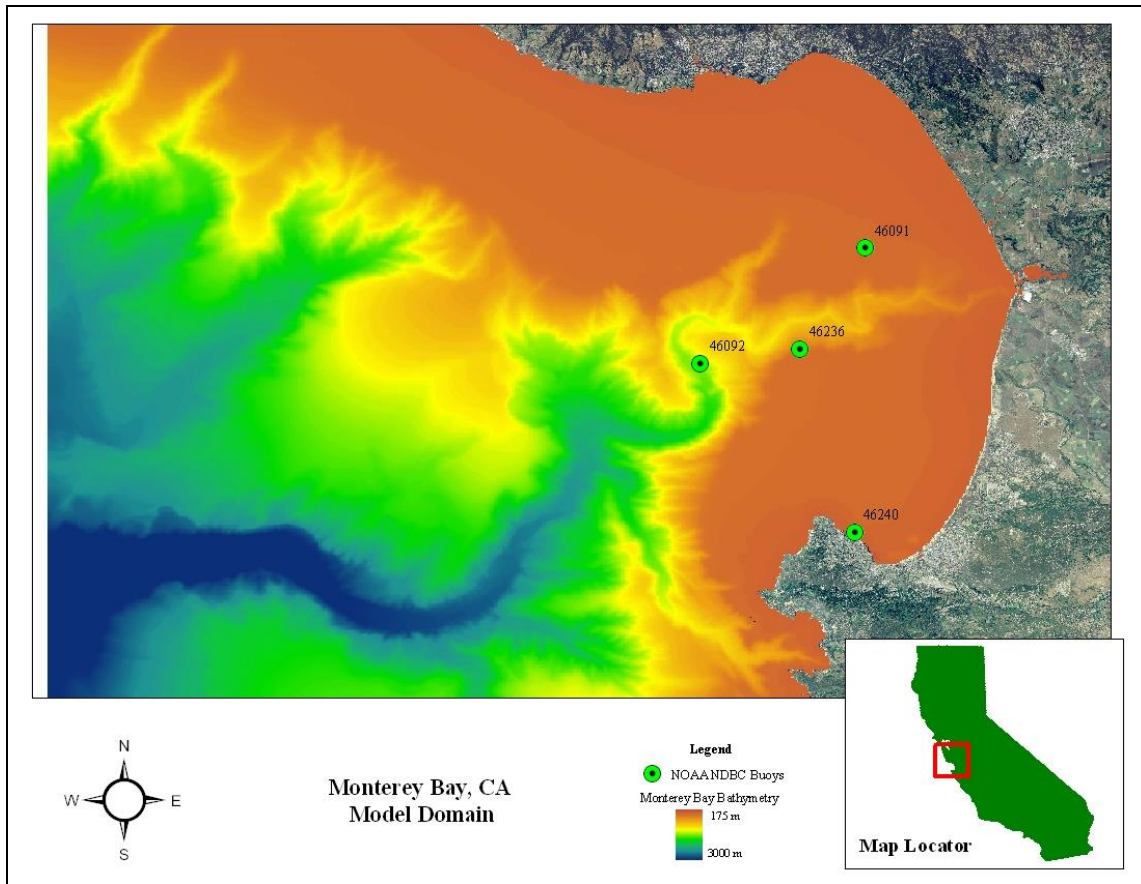


Figure 1. Monterey Bay model domain. NOAA NDBC buoys used for model validation are shown in green.

The Santa Cruz SWAN model domain is shown in Figure 2. A Datawell directional wave buoy (DWR-G) was deployed in the nearshore to measure wave heights, periods, and wave directions during the period of study. The buoy was deployed approximately 100 m south of the Santa Cruz Bight shoreline and used to validate the nearshore model results. A Teledyne/RDI Acoustic Doppler Current Profiler (ADCP) was deployed in proximity to the wave buoy. The ADCP measured water column current magnitude and direction.

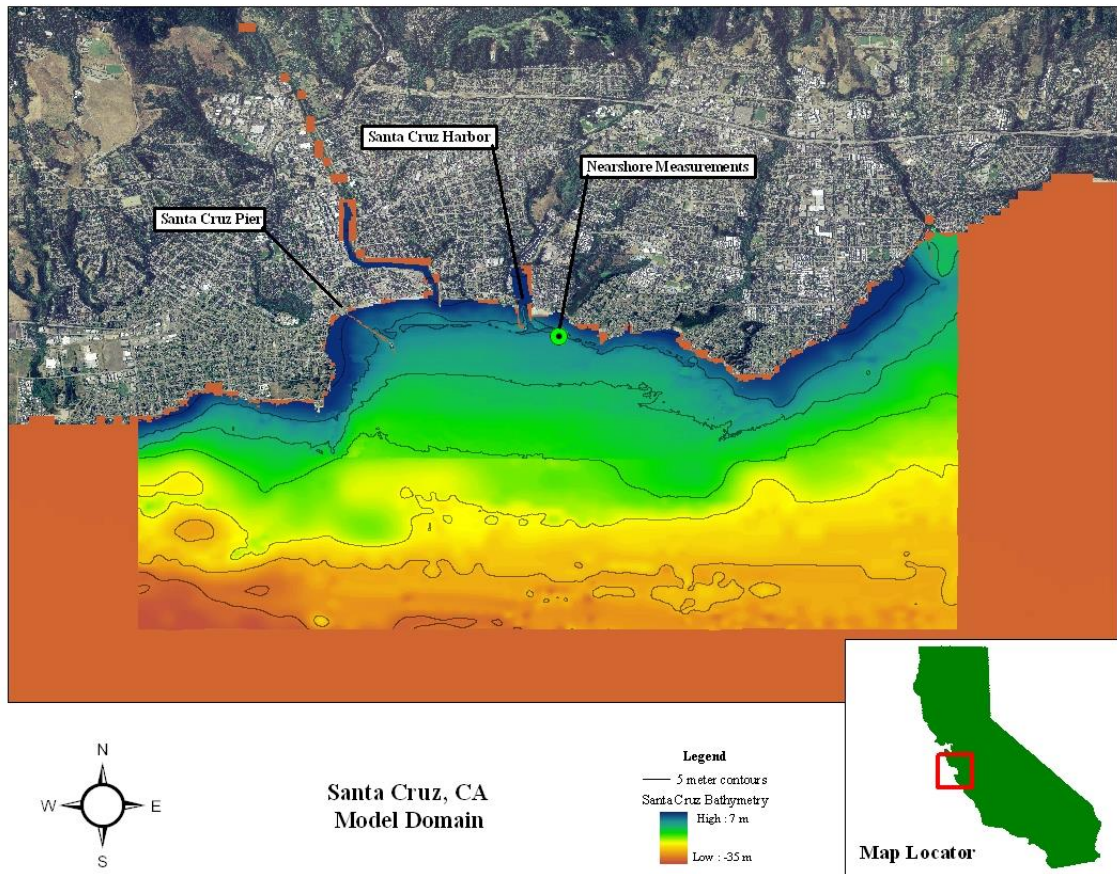


Figure 2. Santa Cruz model domain. Nearshore wave-measurement buoy and bottom-mounted ADCP measurement locations are shown for reference.

2.2. Wave Model Validation

The ability of a wind-wave model to predict wave characteristics can be evaluated in many ways. Here, model performance (modeled versus measured) was assessed through the computation of scatter index (SI), root mean squared error (RMSE), and bias, or mean error (ME). SI (Komen et al., 1994) is defined as the RMSE normalized by the average observed value. ME allows for the detection and evaluation of bias in the wave characteristic data forecasts. When examining results of an ME analysis, a positive value would indicate the average over-prediction of an observed value while a negative value indicates average under-prediction. Model performance was computed for both SWAN models: the coarse grid Monterey Bay model and the nested, finer grid Santa Cruz model.

2.2.1. Coarse Grid Monterey Bay Model Validation

Wave heights (in meters), peak wave periods (in seconds), and mean wave direction (in degrees relative to True North) were obtained from the Monterey Bay SWAN model for validation with

local NDBC buoys in Monterey Bay. Data were outputted every hour at several discrete buoy locations for direct comparison. NOAA NDBC buoy number 46236 was selected as most representative for comparison due to its central Monterey Bay location. Modeled and measured data during the period of study are compared in Figure 3.

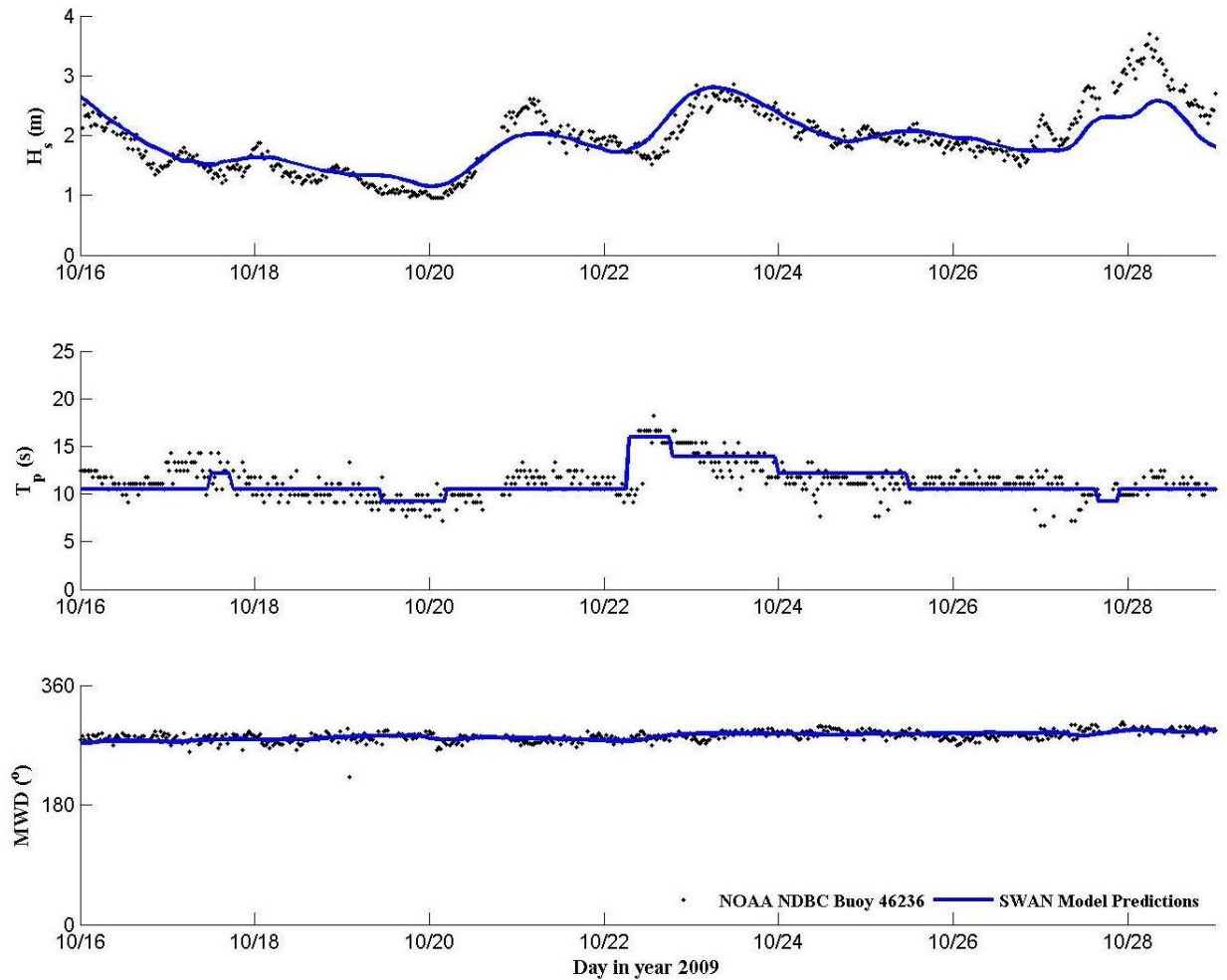


Figure 3. Model (line) representing the wave height (H_s), peak wave period (T_p) and mean wave direction (MWD) obtained from the Monterey Bay SWAN model. Measured data (dots) were obtained from the NOAA NDBC buoy 46236 in Monterey Bay.

The model performance statistics computed from the Monterey Bay SWAN model showed good agreement of modeled to measured data (see Table 1). The wave heights showed $ME = -0.06$ m (i.e., model slightly under-predicts the measured data). The peak periods also showed a slight under-prediction (-0.4 seconds). The mean wave directions were over-predicted by approximately 6° (clockwise) from the measured data. All values were considered within good agreement.

Table 1. Model error statistics for the Monterey Bay SWAN model.

Parameter (units)	RMSE	SI	ME
H _s (m)	0.293	0.174	-0.059
T _p (s)	2.781	0.255	-0.369
MWD (degrees)	21.587	0.077	6.336

2.2.2. *Finer Grid Santa Cruz Model Validation*

Wave heights, peak wave periods, mean wave directions, and total energy dissipation (due to white-capping, wave-breaking, and bottom turbulence) were outputted each hour from the Santa Cruz SWAN model for every grid point in the domain. The wave heights and wave periods were used to assess model performance with measurements from a locally deployed wave buoy. Output parameters (wave heights, radiation shear stresses, and dissipation) were used as input data to the nearshore hydrodynamic model (described below).

Figure 4 is a comparison of model predictions and buoy measurements. The model performance statistics computed from the Santa Cruz SWAN model comparison to measured data also showed good agreement (see Table 2). The wave heights showed a mean error of +0.04 m (slight over-prediction). The peak periods also showed a slight over-prediction of 0.4 seconds. The mean wave directions were under-predicted by 1.5° (counter-clockwise) from the measured data. All model performance values presented here were considered in good agreement. A more detailed description of the data collection effort and model validation conducted for the U.S. Navy is outlined in Chang et al. (2011).

Table 2. Model error statistics for the Santa Cruz SWAN model.

Parameter (units)	RMSE	SI	ME
H _s (m)	0.185	0.218	0.038
T _p (s)	1.197	0.091	0.365
MWD (degrees)	6.916	0.033	-1.53

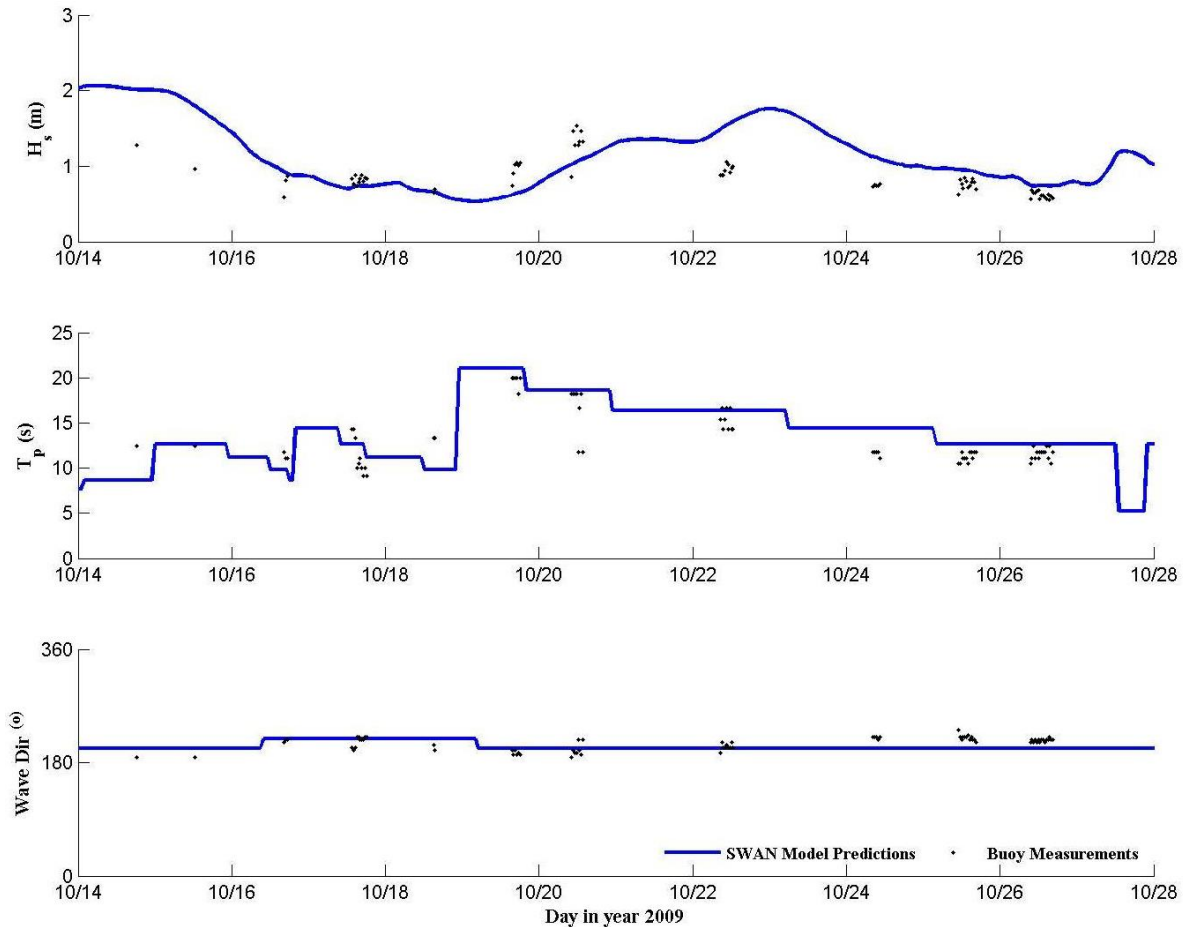


Figure 4. Model (line) representing the wave height (H_s), peak wave period (T_p) and mean wave direction (MWD) obtained from the nearshore Santa Cruz SWAN model. Measured data (dots) were obtained from the Datawell DWR-G buoy deployed during the field study.

2.3. Hydrodynamic Model

The hydrodynamic model, SNL-EFDC, is based on a U.S. EPA approved, state-of-the-art, three-dimensional hydrodynamic model developed at the Virginia Institute of Marine Science by John Hamrick (Hamrick, 1992, 2007a, 2007b), EFDC. EFDC simulates hydrodynamics and water quality in rivers, lakes, estuaries, and coastal regions. The EPA describes the model as “one of the most widely used and technically defensible hydrodynamic models in the world.” SNL-EFDC includes improved hydrodynamics and sediment transport routines (James et al., 2011). This model was selected because it has the following capabilities:

- The model is 3-dimensional, which allows for the simulation of variations in current structure in the vertical as well as horizontal.
- It allows input of nearshore wave-radiation stresses and wave-energy dissipation for simulation of surf zone circulation and transport.

- The model incorporates complex bathymetry.
- The model allows input of time varying flows, winds, water levels, and discharges.

To accurately model transport in the coastal environment, it is critical to describe both the transport and the bottom shear stress. Bottom shear stress controls erosion and deposition and currents are responsible for overall transport. The advective transport flux (q) can be quantitatively calculated by the mass concentration, C , of the substance of interest multiplied by the velocity, u , yielding $q = uC$. Advective flux generally accounts for the majority of transport in coastal systems. Nearshore currents move masses around much more rapidly than diffusive processes. SNL-EFDC handles advective transport through water-column velocities. These velocities are a result of tidal forces, wave forces, and wind.

Diffusive transport is due to molecular and turbulent transport processes. The molecular component is dispersion of a dissolved mass caused by the random motion of molecules in water. The turbulent component of diffusion is the dispersion of mass due to the random motions in the fluid associated with turbulent flow. In coastal systems, turbulent diffusion generally exceeds molecular diffusion rates by many orders of magnitude.

When described mathematically in one dimension, the summation of the advective and diffusive components of transport of a mass concentration (C) into a mass flux (i.e., transport, q) term is:

$$q = uC - K \frac{\partial C}{\partial x}. \quad (1)$$

The second term is where the diffusive transport is quantified and K is the coefficient of turbulent diffusivity. Specification of K is a key component of mass transport and must be considered carefully. The diffusivity must be described in both the vertical and horizontal directions.

Turbulent eddies are responsible for mixing fluid in the water column. In general, the horizontal diffusivity (K_H), responsible for the dispersion of freshwater and/or particles, is proportional to the velocity in the fluid and the physical size of the turbulent eddies. SNL-EFDC uses the Smagorinsky (1963) method to calculate the horizontal diffusivity. The magnitude of the diffusivity in the model is proportional to the horizontal current shear. The Smagorinsky model has been well validated in coastal modeling studies over the past three decades. In addition to the diffusivity due to the current shear, wave dissipation plays a role in K_H . As waves move into shallow water regions, they disperse energy in the form of turbulence (wave dissipation). Wave energy dissipation through generation of turbulence is at a maximum as the wave breaks. This dissipation is calculated in the SWAN wave model and used as an input to SNL-EFDC. Wave dissipation acts as another source of turbulence and is hence added to the K_H determined from the currents in the Smagorinsky model.

Vertical mixing is the product of not only current gradients in the vertical, but also buoyancy gradients. SNL-EFDC implements the Mellor and Yamada (1982) second moment turbulence closure model in the vertical that has been well validated for coastal ocean applications. The model as implemented in SNL-EFDC has been improved and further validated by Galperin et al.

(1988). The Mellor and Yamada model relates vertical turbulent diffusivity to turbulent intensity, turbulent length scale, and the Richardson number (a measure of the buoyancy effects in the flow). Once the vertical diffusivity has been calculated through the Mellor and Yamada model, the wave dissipation from the SWAN model is added as a source of turbulence. Wave dissipation has a much larger relative effect in the vertical than the horizontal and is responsible for significant vertical mixing.

Bottom shear stress, τ_b , is produced at the sediment bed as a result of friction between moving water and a solid bottom boundary. The bottom shear stress is the fundamental force driving sediment transport. Shear stress is denoted as force per unit area (i.e., dynes/cm²). It has been studied in detail for currents and waves, and can be defined and quantified mathematically given sufficient information about the hydrodynamics of the system. Shear stress is responsible for the initiation of sediment transport (i.e., erosion) and the ability of the flow to keep particles in suspension. The calculation of shear stress in areas such as the Santa Cruz region, where waves play a large role, is outlined in more detail by Christoffersen and Jonsson (1985) and Grant and Madsen (1979). The wave- and current-generated bottom shear stresses are calculated in this effort using the Christoffersen and Jonsson (1985) formulation.

The overall modeling approach has limitations that include:

- It is a simplification of a turbulent, chaotic, nearshore process.
- Salinity and temperature gradients are not included at the offshore boundaries. In other words, large-scale ocean circulation is not incorporated into the nearshore region.
- Measurements of currents are only available at nearshore locations for model validation.

Even though the above limitations are considered when assessing the results, this methodology produces accurate estimates of transport due to the dominant nearshore processes in the region (i.e., waves and tides). These can be used to develop quantitative relationships for sediment transport in the vicinity of marine hydrokinetic (MHK) devices and to assess the forces acting directly on the MHK devices.

2.3.1. Site-Specific Hydrodynamic Model: Monterey Bay and Santa Cruz, CA

The initial development of the SNL-EFDC model required input of the regional coastal bathymetry. The bathymetry in the project area was derived from high-resolution bathymetric data. Bathymetry was represented in the numerical model through the creation of a grid and the specification of depth at each cell center. Grid dimensions were selected to balance desired resolution and computational cost. Figure 5 shows the site bathymetry interpolated onto the model grid. The grid cell size was 20×20 m², and the overall grid dimensions were 4.9 km in the alongshore direction (Point Santa Cruz to Soquel Point) and 3 km in the onshore-offshore direction.

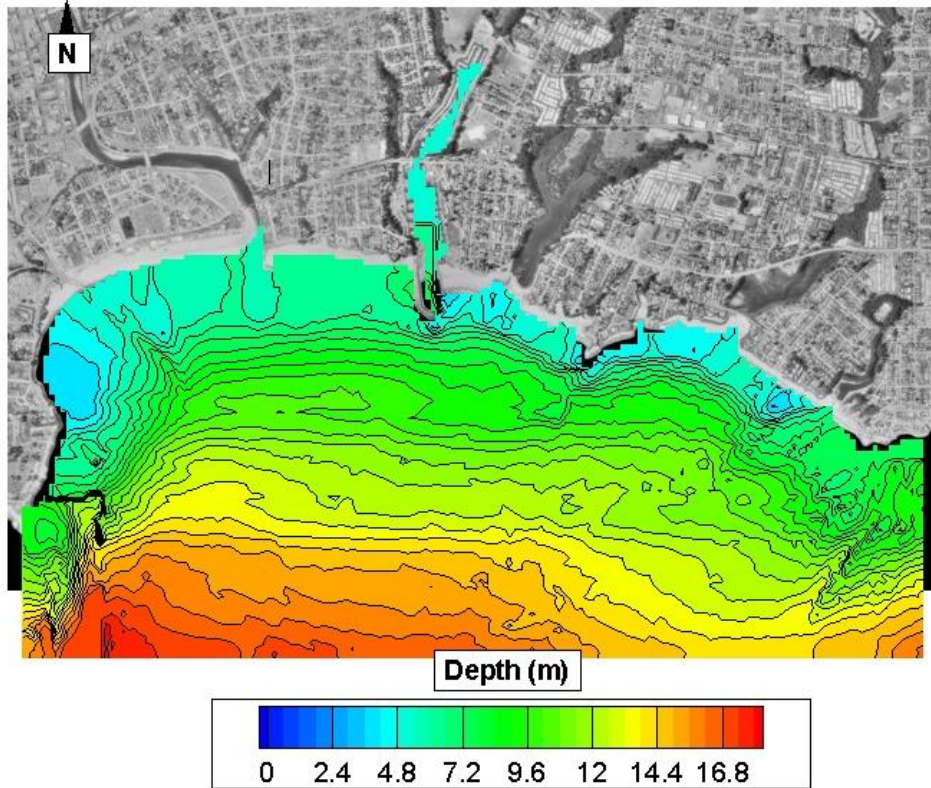


Figure 5. Contours of bathymetry mapped to 20 m x 20 m SNL-EFDC grid for the Santa Cruz region.

The tidal water-level variations corresponding to the conditions in October 2009 were used as model boundary conditions. The water level was applied along the east boundary of the grid. The tidal water level variations were determined from the NOAA CO-OPS (Center for Operational Oceanographic Products & Services) values for tides in the Santa Cruz region (<http://co-ops.nos.noaa.gov/index.html>). In addition, from the CO-OPS tidal information and the measured currents information, tidal propagation along the Santa Cruz coast was typically from east to west; therefore a tidal lag time was applied to the water levels along the west model boundary. Wind conditions over the model region were assumed to be equivalent to the conditions measured at the Santa Cruz Municipal Wharf, which was central in the model domain. The hourly measured wind speed and direction from the wharf were applied over the entire model domain for the month of October 2009. Figure 6 shows both the water levels and winds for October 2009.

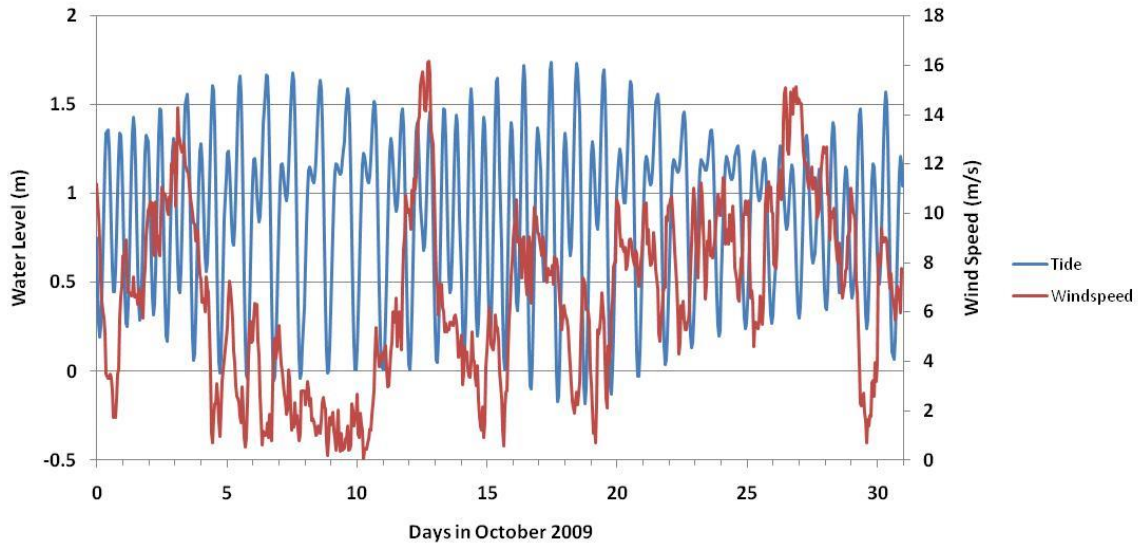


Figure 6. Tidal water levels and winds applied as model boundary conditions for the Santa Cruz model.

2.4. Hydrodynamic Model Validation

To ensure that the model accurately simulated currents in the project area, actual currents measured by the current meter were compared with those simulated using the wave, tide, and wind boundary conditions. The SWAN model was run for the entire field data collection period to produce time series of wave parameters for the entire model domain. These results were incorporated into the SNL-EFDC model for the time period of interest with the actual tide and winds applied to the domain.

The SWAN modeled peak wave heights on 10/14/2009 are shown in Figure 7 mapped onto the SNL-EFDC grid. Figure 8 and Figure 9 show the wave heights and resulting shear stresses, and velocity contours from SNL-EFDC overlaid in the study area. These results demonstrated that along-shore velocities to the east are occurring in the region. In addition, the combined wave and current shear stresses and velocities provided the fundamental physical parameters for sediment transport studies under this task.

A quantitative comparison of measured data over the 4 days for which measurements were available to modeled nearshore, depth-averaged current magnitude data for the Santa Cruz nearshore currents model is presented in Figure 10. Table 3 lists the model performance indicators. On average, the model under-predicted the currents by less than 1 cm/s, which was within the 1.5 cm/s velocity error in the ADCP measurements. The combined wave and current model agreement with the measurements was considered excellent. Additionally, the results show along-shore velocities to the east consistent with drifter observations and ADCP measurements made during the field measurement period.

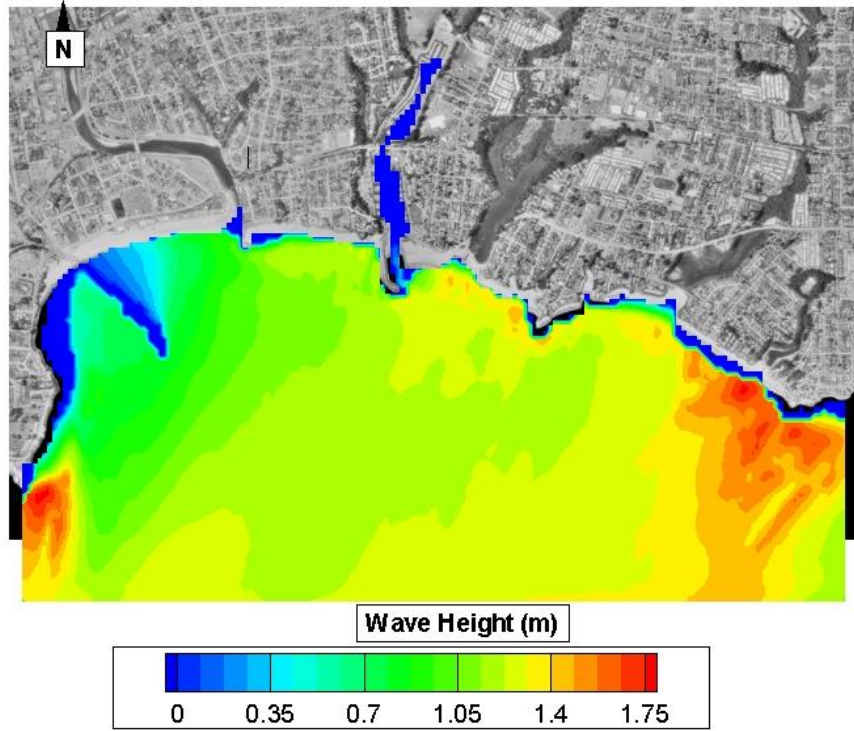


Figure 7. Significant wave heights from the SWAN model in the SNL-EFDC model domain on 10/14/2009.

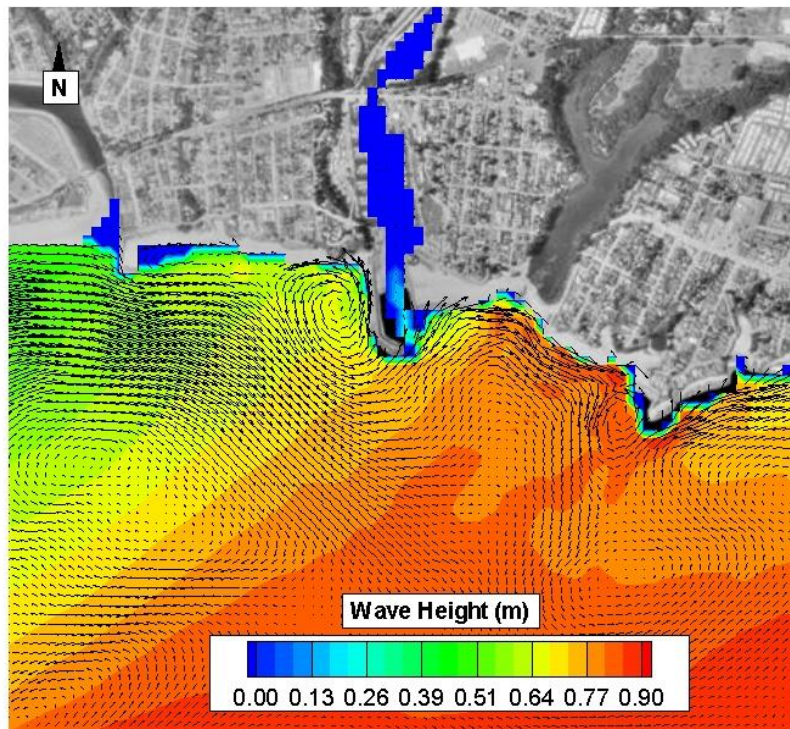


Figure 8. Peak wave heights and velocity vectors in the model domain on 10/14/2009.

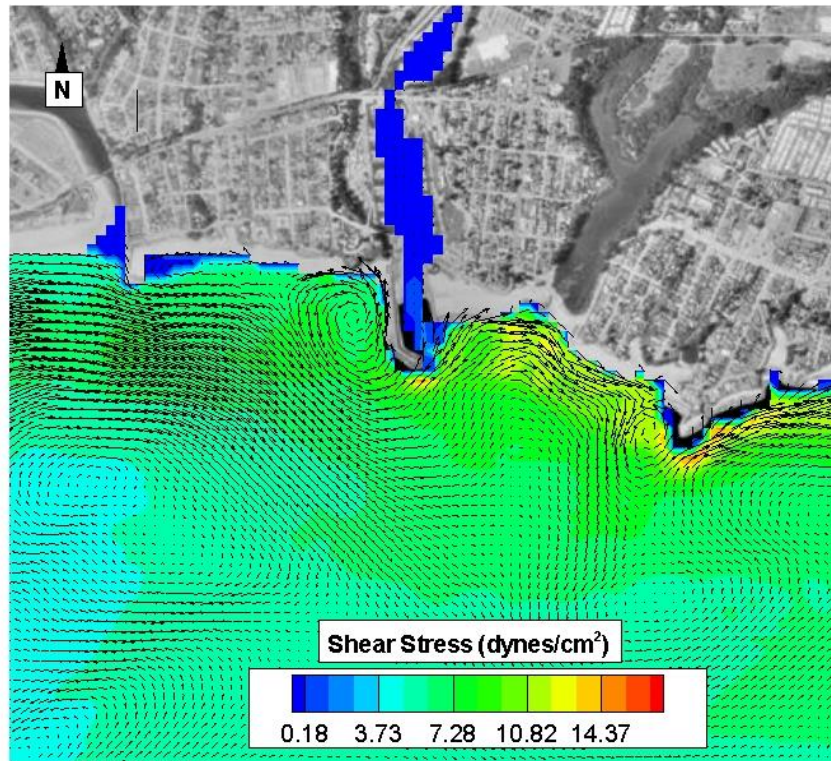


Figure 9. Combined wave and current shear stresses and velocity vectors in the model domain on 10/14/2009.

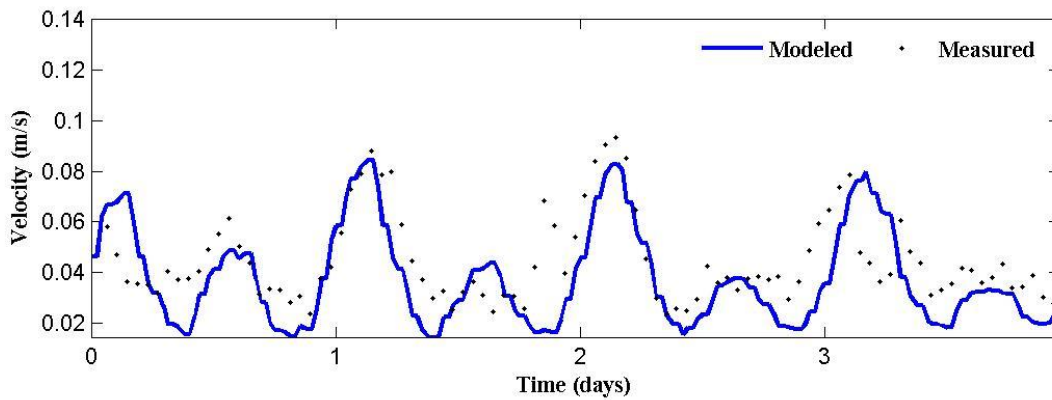


Figure 10. Model (line) representing the current magnitude obtained from the nearshore Santa Cruz SNL-EFDC model. Measured data (dots) were obtained from the Teledyne RDI ADCP deployed during the field study.

Table 3. Model error statistics for the Santa Cruz combined wave and current model.

Parameter (units)	RMSE	SI	ME
Velocity (m/s)	0.016	0.361	-0.008

3. SIMULATION OF WEC ARRAY

The goals of the present effort were to develop and apply tools to quantitatively characterize the environments where WEC devices may be installed and to assess alterations to hydrodynamics and local sediment transport caused by WEC operation. In this study, WEC devices were simulated in the SWAN model as discrete obstructions to the propagating wave energy and the subsequent wave fields were passed to the SNL-EFDC model as described above. For the investigation here, the modeled WEC array consisted of 200 individual WEC devices organized into a honeycomb shape similar to proposed point absorber arrays (Figure 11). The center of the array was placed at the 40 meter depth contour; about 4 miles off the coast in the predominant wave direction. The WEC devices were modeled as 25 meter diameter structures spaced approximately 50 meters center-to-center. The distance between device edges was, therefore, approximately 40 meters. The hydrodynamics and sediment transport domain, discussed in the following sections, was focused on the nearshore where the largest potential effects are anticipated. The area of this domain is highlighted in Figure 11.

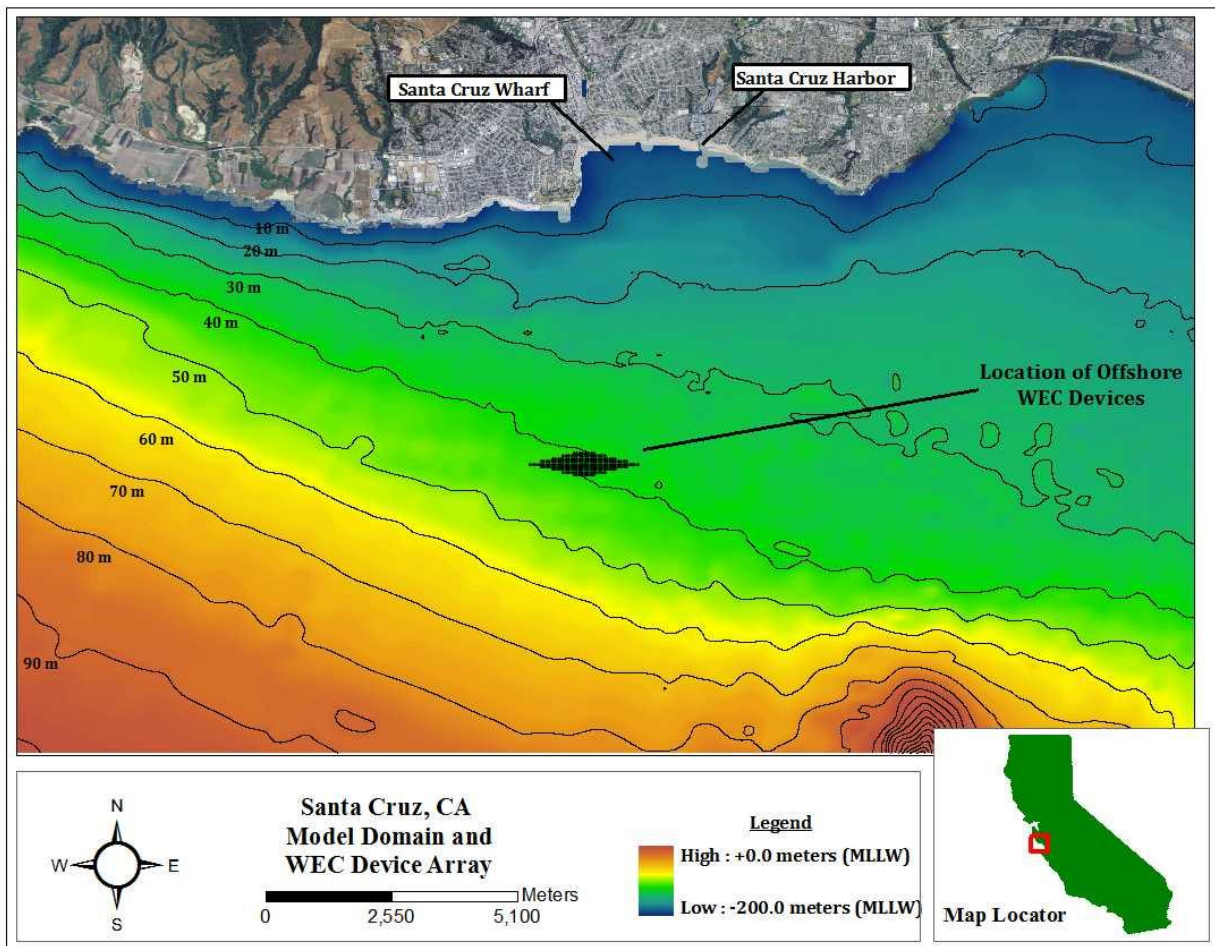


Figure 11. Near-shore Santa Cruz, CA, model bathymetry and WEC device array location.

3.1. Wave Model with WECs

An environmentally conservative scenario was assumed for these simulations to evaluate the perceived largest potential effects of a WEC array on the local wave environment. Recent laboratory observations of wave propagation past a WEC array has indicated that “wave absorption is the dominant process inducing the wave shadow” (Haller et. al., 2011). As such, no wave energy was reflected from the WEC array within SWAN, while 100% of the wave energy was absorbed by the devices. This created a wave shadowing effect in lee of the array. The accuracy of this simple technique for simulating WEC arrays is unknown at present.

Two wave cases were used for the simulations: (1) a significant wave height of 1.7 m with a peak period of 12.5 s was used as the average condition and (2) storm conditions were represented by the 95th percentile wave height of 3.5 m with a period of 17 s. The direction of the peak yearly wave energy was from the northwest. These cases were used as general representations of average and extreme conditions. The modeled wave heights for the 1.7 m average wave case before and after WEC array installation are illustrated in Figure 12 and Figure 13. It is clear that inclusion of devices that inhibit wave transformation caused wave heights to be reduced behind the devices. This was due to the absorption (and resultant conversion into power) of wave energy by the WEC devices. The change in wave patterns as a result of the obstructions was incorporated into the hydrodynamic model and subsequent sediment transport model.

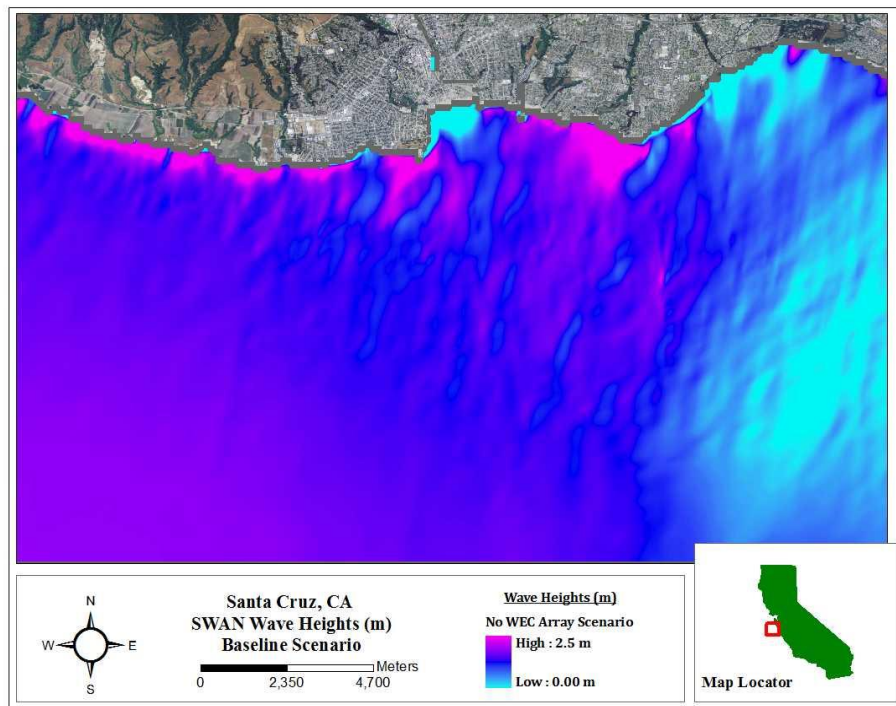


Figure 12. Modeled wave heights prior to the installation of a WEC device array.

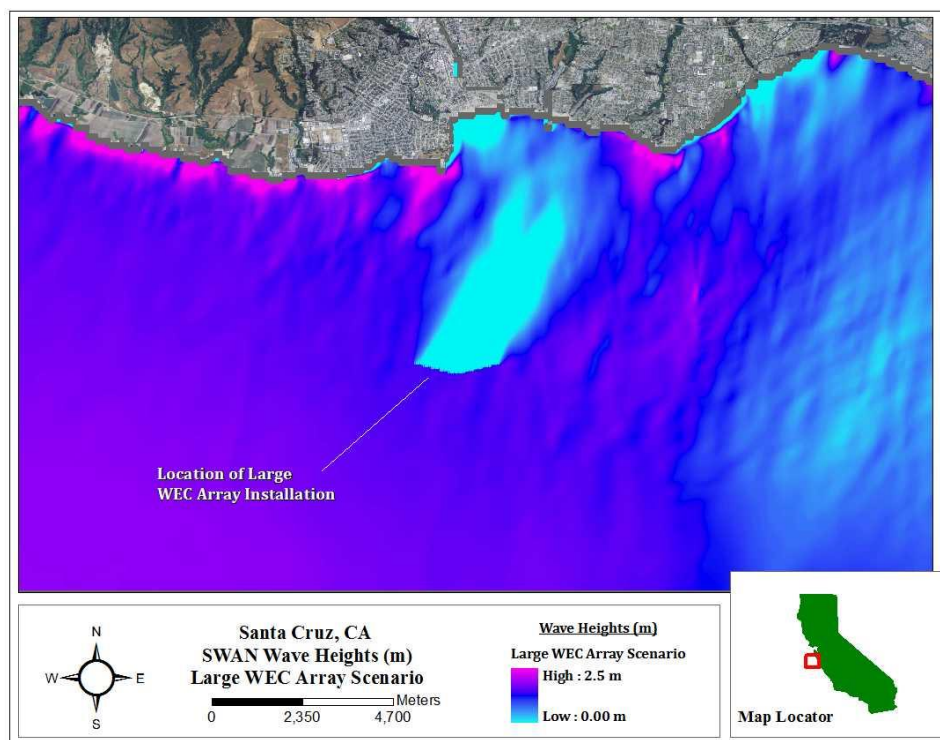


Figure 13. Modeled wave heights after installation of a WEC device array for an incoming wave height of 1.7 m.

3.2. Hydrodynamics and Sediment Transport Models with WECs

Wave orbital velocities and wave-driven and tidal currents are among some of the predominant forcing mechanisms in near-shore regions. The combined forcing mechanisms cause shear stresses at the sediment-water interface. When the shear stresses are large enough, individual sediment particles will begin to mobilize, and may travel in bedload (along the seafloor) or become suspended in the water column and be transported with the ambient current. Waves are the primary source of shear stress at the sediment bed in the near-shore region that can cause resuspension of sediment; however, once suspended, sediments will be transported by the combined currents produced by waves and tides. Therefore, calculation of the shear stresses as a result of combined wave-current interactions, which is conducted in SNL-EFDC, is necessary to truly represent the expected near-bed forces. It should also be noted that in nearshore regions sediment transport patterns are dynamic and nearly always active. The interest in the present modeling study was to determine the change in the patterns of the sediment dynamics due to the presence of WEC devices.

The SNL-EFDC model was run for a one week period with the average and extreme SWAN wave characteristics incorporated. The SNL-EFDC model was run with the same tidal boundary conditions as validated in the October 2009 Santa Cruz, CA case to provide a comparable validated baseline. There was little variation yearly in the semi-diurnal spring-neap tidal cycle,

so the waves were the primary forcing for evaluation. For the sediment transport simulations, the average (1.7 m wave height) and extreme (3.5 m wave height) were used.

Near-bottom shear stresses were computed due to the combined wave and currents from SNL-EFDC model following the method of Christoffersen and Jonsson (1985), which accounts for the ambient current velocities, wave-induced orbital velocities and seabed roughness. Changes in sediment transport patterns were investigated using SNL-EFDC. The SNL-EFDC model took into account multiple sediment size classes, has a unified treatment of suspended load and bedload, and describes bed armoring. The sediment transport model maintained a physically consistent treatment of bedload and suspended load, which was ideally suited to the coastal nearshore environment. Experimental data from a sand sized sediment erosion experiment in a straight channel helped validate the numerical model. Sampling efforts conducted by the United States Geological Survey (USGS) and Santa Cruz Port District were used to develop grain size maps of the model region. For these initial investigations, the grain size distribution comprised of three separate size classes to define the initial sediment conditions. The size classes consisted of 200, 1000, and 3000 μm sediment representative of fine, medium, and coarse sand and the bed was initially comprised of equal portions of each (Table 4).

Table 4. Sediment size class properties.

Class	Particle Diameter (μm)	Settling Speed (cm/s)	Initial Sediment Bed Fraction
Fine Sand	200	1.5	0.34
Medium Sand	1000	9.9	0.33
Very Coarse Sand	3000	20.9	0.33

Figure 14 shows a zoomed view of the modeled circulation patterns and resultant change in sediment bed height both before (baseline scenario) and after installation of the WEC array for the larger 3.5 m wave case (i.e. extreme). A zoomed view was used here to highlight specific circulation patterns in areas affected by the WEC devices. Evaluations of the entire model domain are presented in following figures. It is important to note that these results did not represent a steady-state after the one week period, but were representative of dynamic patterns of overall transport.

The baseline results produced behavior consistent with observed nearshore circulation in the Santa Cruz region. The overall circulation and sediment transport were in a "down-coast" or easterly direction. The transport was divided into cells by the numerous rocky points in the region that are erosional (blue), while the beach regions retain sand (red). The blue streaks offshore were also observed in large scale multi-beam surveys of the area as transporting sand waves. The consistency of these results contributed to the overall reliability of the model.

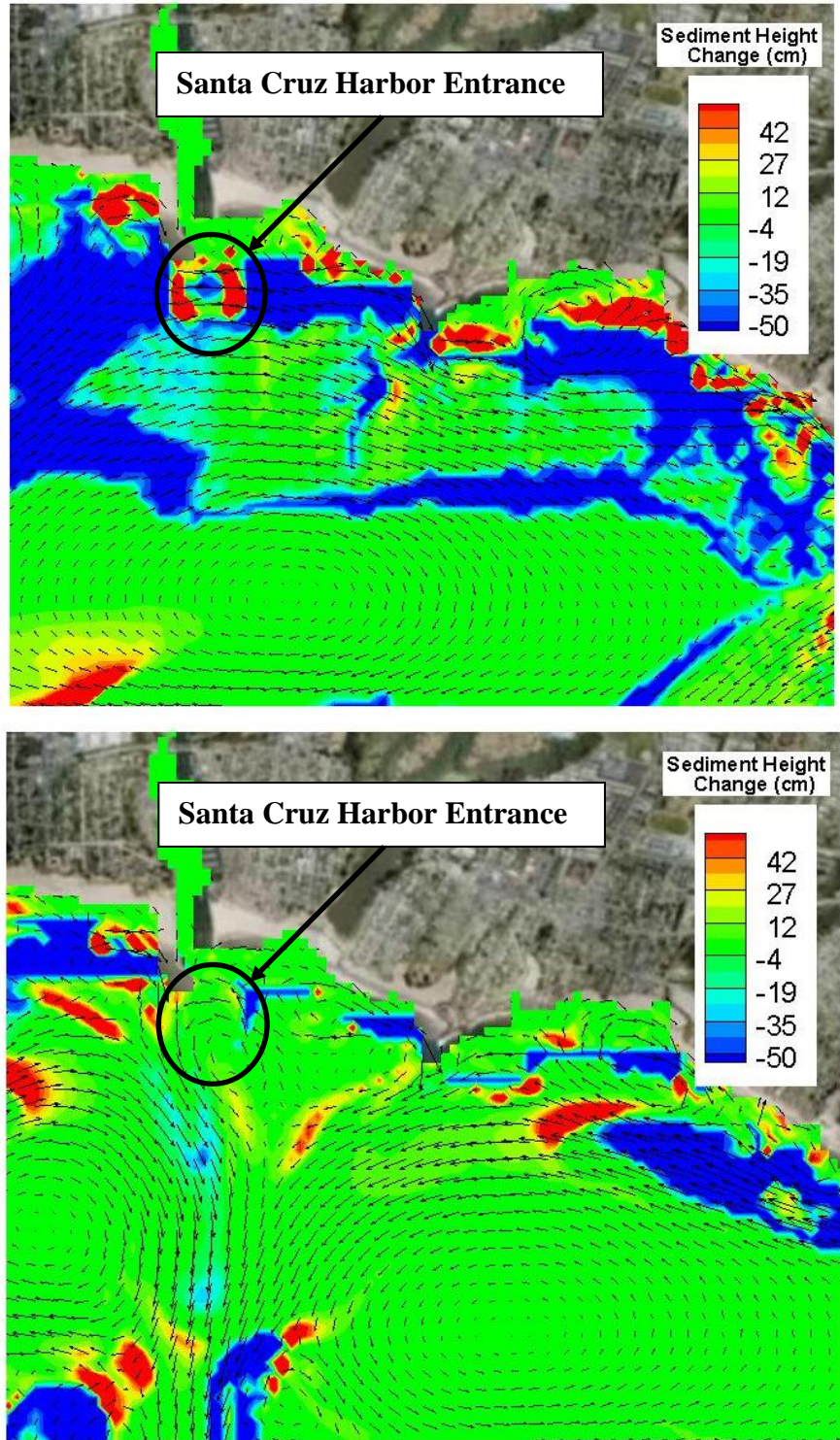


Figure 14. Velocity vectors and resultant sediment bed height change in cm from the combined wave and circulation model for the 3.5 m wave case. The top panel illustrates the baseline case and the bottom panel shows the case with the offshore WEC array in place.

Overall, the WEC array case showed less change in the sediment bed and a disruption of the common easterly currents developed in the nearshore region of Santa Cruz. The circulation in the lee of the array was also altered; reduction of energy in this region created large offshore flow to balance the higher wave energy up and down the coast during the storm event. The disruption of circulation patterns can alter water quality and seasonal sediment transport patterns that must be investigated on a site specific basis. The implications of these results are discussed further in the next section; however the comparison of the sediment bed height changes showed that there was a quantifiable effect on circulation patterns and sediment transport in the nearshore due to the presence of the offshore WEC array.

To better illustrate the changes associated with the presence of a WEC array, the sediment bed heights and particle size distributions were investigated as indicators of overall effect. By subtracting the baseline results from the results of the WEC array, a difference in the two cases were evaluated. The difference in sediment height illustrates the net erosion or deposition induced by the WEC array, while the difference in particle size illustrates the increase or decrease in surface particle size. Figure 15 shows the difference in sediment bed height and change in surface sediment particle size from the model for the 1.7 m wave height during the normal tide cycles. Coarser particle sizes or erosion generally indicated higher energy, while smaller particles or deposition indicated lower energy regions. In general, it was evident that the WEC installation allowed for more deposition; however there was a complex interplay that resulted in "hot spots" of sediment mobility. The results indicated that there was a significant increase in finer sediment sizes in lee of the WEC array. One reason for this was a decrease in wave heights (decrease in wave orbital velocities) in lee of the array. A second reason was a change in current circulation as a result of the decreased wave energy in lee of the array. The region where the array was located also showed increased fine material in the sediment bed due to the reduced energy adjacent to the array.

Figure 16 shows the difference in sediment bed height and change in surface sediment particle size from the model for the 3.5 m storm wave height. The larger waves mobilized much more sediment than the previous case and the difference plot shows that in general, the WEC installation allowed for more deposition of any mobilized sediment, yet in the very nearshore to the east of the harbor excess sediment erosion was seen. This was potentially due to the disruption of sediment supply to these areas during larger events that would normally inhibit erosion. The particle sizes decreased substantially offshore consistent with an overall reduction of wave energy and shear stress in the region allowing finer particles to accumulate at the surface. An unanticipated effect was the reduction of sediment deposition in the harbor mouth that could have a benefit of reducing dredging quantities required after large winter storms.

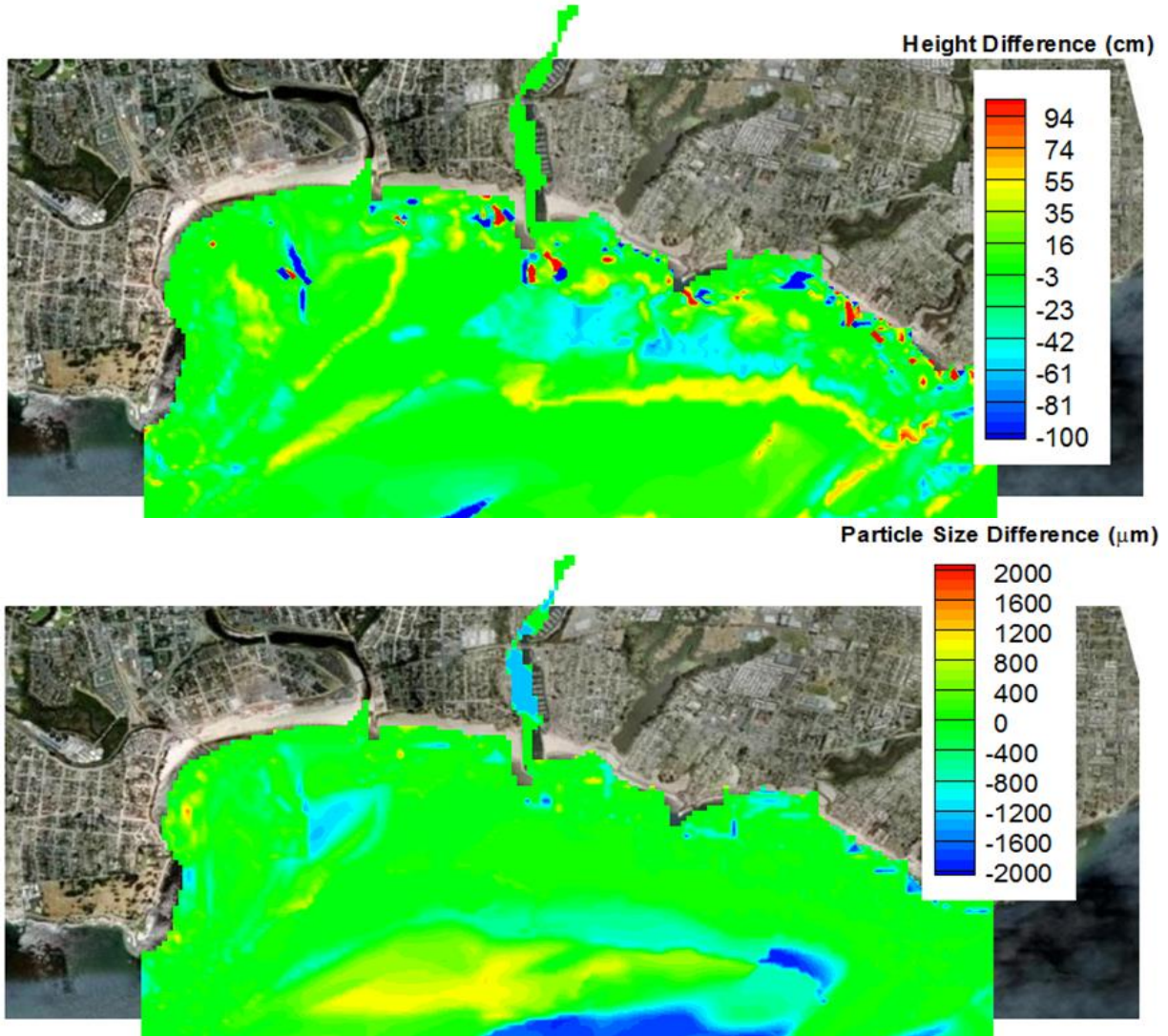


Figure 15. Differences between the combined wave and circulation baseline model and WEC array model after 4 days of 1.7 m waves and normal tides. The top panel illustrates the change in sediment bed height and the bottom panel shows the change in sediment surface particle size.

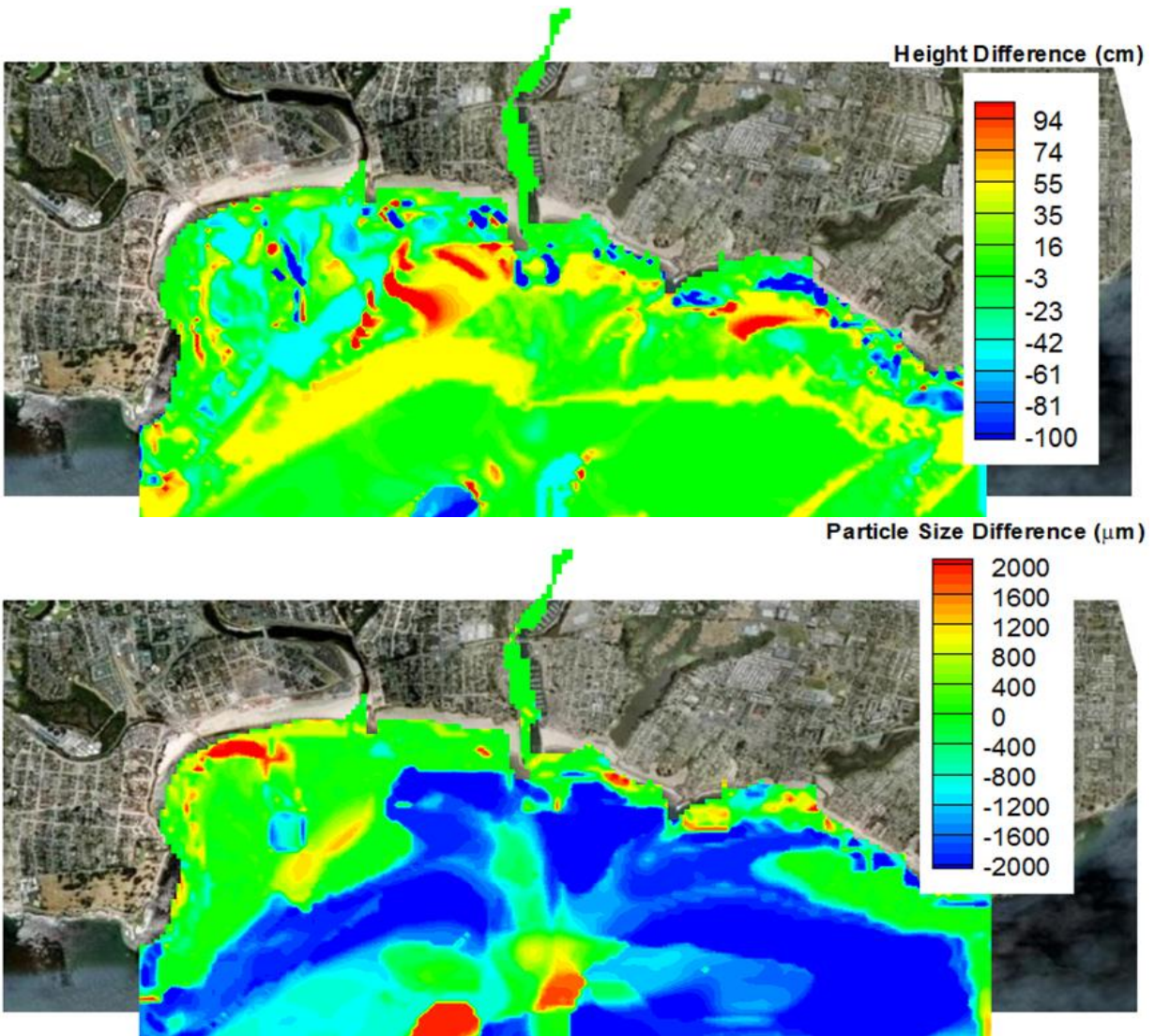


Figure 16. Differences between the combined wave and circulation baseline model and WEC array model after 4 days of 3.5 m waves and normal tides. The top panel illustrates the change in sediment bed height and the bottom panel shows the change in sediment surface particle size.

4. DISCUSSION AND CONCLUSIONS

The goal of this study was to develop tools to quantitatively characterize the environments where WEC devices may be installed and to assess effects of WECs on hydrodynamics and local sediment transport. The SWAN wave model coupled with the SNL-EFDC hydrodynamic model developed for the Santa Cruz coast showed excellent agreement with predictions. The comparative model-to-measurement metrics showed that the models accurately reproduced the wave heights and currents in the nearshore region. When incorporated into the SNL-EFDC hydrodynamic model, the waves drove current magnitudes and directions consistent with observations in each study area.

The large hypothetical WEC array investigated in the modeling study did show significant alterations to the wave and circulation properties. The SNL-EFDC sediment transport model was applied to investigate the potential effect of the changes. Differences in surface particle size between baseline (no WECs) and the WEC array simulations were used as a direct indicator of effects to the nearshore region. The results indicated that there was a significant increase in finer sediment sizes in the lee of the WEC array. The region where the array was located also showed increased fine material in the sediment bed due to the reduced energy adjacent to the array. The circulation in the lee of the array was also altered, where more intense onshore currents were generated in the lee. The behavior was created by a low energy zone in the lee of the array bounded by large waves on either side. The balance of energy in this region created large onshore flow. The disruption of circulation patterns can alter water quality and seasonal sediment transport patterns that can be investigated, using this general approach, on a site specific basis. In general, the storm wave case and the average case showed the same qualitative patterns, suggesting that these trends would be maintained throughout the year. The changes were significantly increased during larger storm events where bed height changes were over 1 m and particle sizes changed from coarse sands greater than 2000 μm to fine sand sizes consisting of 200 μm particles.

The modeling framework of SWAN and SNL-EFDC combined with field validation datasets allowed for a robust quantitative description of a nearshore environment within which MHK devices were evaluated. This quantitative description can be directly incorporated into environmental impact assessments and eliminate the guesswork as to the effects of the presence of large scale MHK arrays. It is important to emphasize that in this analysis, all WEC devices were modeled using simple obstruction functions within SWAN that utilize *transmission* and *reflection* coefficients. Recently, laboratory wave tank data have been made available for model calibration and validation of wave propagation around 1, 3, and 5 point absorber-like WEC devices. For the present study, an environmentally conservative approach (100% energy extraction) was used to represent WEC obstruction to wave propagation. This was considered environmentally conservative because physical environmental changes were expected to increase as more energy was removed from the propagating waves by WEC devices. As SNL makes progress on more realistic WEC representations, those representations will be included into future modeling efforts.

The array scenario and WEC representation presented here signified a potential ‘worst case scenario’. It has been postulated that realistic transmission coefficients may be in the range of 30

to 50%. However, based on the results herein, even with absorption cut in half (50%), deploying 200 WEC devices 6 km (4 miles) offshore will create a wave shadow with a noticeable effect on nearshore wave and circulation processes and potentially a measureable ecological footprint. The WEC spacing, absorption, and general placement offshore are all important factors to consider when evaluating the effects of WEC arrays on nearshore processes. The general framework developed here can be used to design more efficient arrays while minimizing impacts on nearshore environments.

Investigating additional array scenarios and more accurately representing the influence of WEC device operation on wave propagation are the next steps in furthering the utility of this analysis. Modifying SWAN accurately and validating with laboratory data sets requires a significant technical effort. In the interim, it is worthwhile to validate the sediment transport models. The sediment transport simulations presented here provided a means with which to compare the relative effect of WEC arrays on nearshore processes. Supplementary work can be done to validate baseline (without WECs) sediment transport behavior. An important task is developing initial sediment conditions that contain realistic spatial distributions of sediment types throughout the domain, including the identification of bedrock. Presently available data include:

- Repeated multi-beam surveys in the fall of 2006 conducted to determine change in seabed properties and surface grabs of sediment for particle size analysis (Santa Cruz Port District).
- Nearshore measurement of waves and currents collected for model validation in 2006 (Santa Cruz Port District).
- Nearshore measurement of waves and currents collected for model validation in 2009 (CEROS).
- High resolution multi-beam survey to evaluate seabed habitat conducted in 2009 (USGS)

These datasets provide readily available information for the setup, calibration, and validation of the SNL sediment stability model. The datasets and model will also be used to determine data gaps that may inhibit model development at other sites. These may include:

- Sediment cores for erosion analysis.
- Collocated wave and current information to investigate seasonal differences.
- Further high resolution surveys to identify long term changes.

These efforts will help provide a complete database for model validation so that critical data needs can be identified and non-critical data eliminated. The effort will lend credibility to the tool and methodology and increase industry confidence in the tool through this initial demonstration.

5. REFERENCES

1. Chang, G., C. Jones, D. Hansen, M. Twardowski, and A. Barnard, *Prediction of optical variability in dynamic nearshore environments*, Technical Report, SEI 11-01, Santa Cruz, CA, 1998.
2. Cristoffersen, J. and I. Jonsson, *Bed friction and dissipation in a combined current and wave motion*, *Ocean Engineering*, 17(4), 479-494, 1985.
3. Galperin, Y. M., V. L. Gurevich, and D. A. Parshin, *Nonlinear resonant attenuation in glasses and spectral diffusion*, *Physical Review B*, 37(17), 10,339, 1988.
4. Grant, W. D. and O. S. Madsen, *Combined wave and current interaction with a rough bottom*, *Journal of Geophysical Research*, 84(C4), 1797-1808, 1979.
5. Haller, M. C., A. Porter, P. Lenee-Bluhm, K. Rhinefrank, and E. Hammagren, *Laboratory Observations of Waves in the Vicinity of WEC-Arrays*, Proceedings of the 9th European Wave and Tidal Energy Conference Series, Southampton, UK, 2011.
6. Hamrick, J. M., *A Three-Dimensional Environmental Fluid Dynamics Computer Code: Theoretical and Computational Aspects*, Virginia Institute of Marine Science, The College of William and Mary, 1992.
7. Hamrick, J. M., *The Environmental Fluid Dynamics Code: Theory and Computation*. In: I. Tetra Tech (Ed.), (Vol. 1-3), US EPA, Fairfax, VA, 2007a.
8. Hamrick, J. M., *The Environmental Fluid Dynamics Code: User Manual*, In: I. Tetra Tech (Ed.), US EPA, Fairfax, VA, 2007b.
9. Komen, G. J., L. Cavaleri, M. Doneland, K. Hasselmann, S. Hasselman, and P. A. E. M. Janssen, *Scatter index*, Cambridge University Press, Cambridge, UK, 1994.
10. Mellor, G. L. and T. Yamada, *Development of a turbulence closure model for geophysical fluid problems*, *Reviews of Geophysics and Space Physics*, 20(4), 851-875, 1982.
11. Smagorinsky, J., *General circulation experiments with the primitive equations I. The Basic Experiment*, *Monthly Weather Review*, 91(3), 99-164, 1963.

DISTRIBUTION

4 Lawrence Livermore National Laboratory
Attn: N. Dunipace (1)
P.O. Box 808, MS L-795
Livermore, CA 94551-0808

1 MS0899 Technical Library 9536 (electronic copy)



Sandia National Laboratories